SCA3_fin.doc 5 Fig, 1 Table, 3 Sup Figs, text 3,112 words, Abstract 140 words
December 9, 2007

Deranged calcium signaling and neurodegeneration in spinocerebellar ataxia type 3

Xi Chen[1], Tie-Shan Tang[1], Huiping Tu[1$], Omar Nelson[1], Mark Pook[2], Robert Hammer[3], Nobuyuki Nukina[4], Ilya Bezprozvanny[1#]

[1]Department of Physiology, [3]Dept of Biochemistry, UT Southwestern Medical Center at Dallas, Texas, USA,
[2]Division of Biosciences, School of Health Sciences and Social Care, Brunel University, Uxbridge, United Kingdom,
[4]Molecular Neuropathology Group, RIKEN Brain Science Institute, Saitama, Japan

Key words: calcium signaling, neurodegeneration, ataxin-3, spinocerebellar ataxia type 3, SCA3, Machado-Joseph disease, MJD1, transgenic mouse, stereology, dantrolene

*Corresponding author:
Dr. Ilya Bezprozvanny
tel: (214) 645-6017
fax: (214) 645-6018
E-mail: Ilya.Bezprozvanny@UTSouthwestern.edu

[$]Present address: Department of Cardiovascular Disease, Merck research laboratories, PO Box 2000, Rahway, NJ 07065-0900.

Robert.Hammer@UTSouthwestern.edu

nukina@brain.riken.jp

Mark.Pook@brunel.ac.uk

huiping_tu@merck.com

Acknowledgments

We thank Xiangmei Kong and Tianhua Lei for help with maintaining the SCA3 mouse colony, Janet Young for administrative assistance, Noelle Williams for assistance with the measurements of dantrolene concentrations, Lisa Monteggia, Jenny Hsieh, Malu Tansey, Keith Tansey and Don Cooper for help and advice with behavioral and stereological experiments. IB is supported by the Robert A. Welch Foundation, National Ataxia Foundation, Ataxia MJD Research Project, the McKnight Endowment Fund for Neuroscience, and NINDS grants R01NS38082 and R01NS056224. ON is suported by DCMB training grant. MP is supported by Ataxia, UK and Ataxia MJD Research Project. NN is supported by grant-in-aid from MEXT of Japan (17025044)

Abstract

Spinocerebellar ataxia type 3 (SCA3), also known as Machado-Joseph disease (MJD), is an autosomal-dominant neurodegenerative disorder caused by a polyglutamine expansion in ataxin-3 (SCA3, MJD1) protein. In biochemical experiments we demonstrate that mutant $SCA3^{exp}$ specifically associated with the type 1 inositol 1,4,5-trisphosphate receptor ($InsP_3R1$), an intracellular calcium (Ca^{2+}) release channel. In electrophysiological and Ca^{2+} imaging experiments we show that $InsP_3R1$ are sensitized to activation by $InsP_3$ in the presence of mutant $SCA3^{exp}$. We found that feeding SCA3-YAC-84Q transgenic mice with dantrolene, a clinically relevant stabilizer of intracellular Ca^{2+} signaling, improved their motor performance and prevented neuronal cells loss in pontine nuclei and substantia nigra regions. Our results indicate that deranged Ca^{2+} signaling may play an important role in SCA3 pathology and that Ca^{2+} signaling stabilizers such as dantrolene may be considered as potential therapeutic drugs for treatment of SCA3 patients.

Introduction

Spinocerebellar ataxia type 3 (SCA3), also known as Machado-Joseph disease (MJD), is an autosomal-dominant neurodegenerative disorder that belongs to a group of polyglutamine (polyQ)-expansion diseases [1-3]. The symptoms of SCA3 include gait ataxia, dysarthria, dysmetria, hyperreflexia, dystonia and ophthalmoplegia [4]. The brain regions most affected in SCA3/MJD are dentate and pontine nuclei, internal portion of globus pallidus, sub-thalamic nucleus, substantia nigra, and spinocerebellar tracts [5]. At molecular level the cause of SCA3 is a polyQ expansion in the carboxy-terminal of ataxin-3 (SCA3, MJD1) protein [6,7]. The ataxin-3 is a 43 kDa cytosolic protein that contains amino-terminal Josephin domain and 2 ubiquitin-interactions motifs [8,9]. PolyQ-expansion occurs in carboxy-terminal region of ataxin-3 that does not contain any known functional motifs. Despite intense efforts, the cellular pathogenic mechanism of SCA3 remains unclear.

Huntington's disease is another member of polyQ-expansion disease family, which is caused by a polyQ-expansion in the context of Huntingtin protein (Htt). In our previous studies we demonstrated that mutant Htt^{exp} protein specifically binds to and activates type 1 inositol 1,4,5-trisphosphate receptor ($InsP_3R1$) [10]. From these results we proposed that deranged Ca^{2+} signaling may play an important role in HD pathogenesis [11]. These ideas were supported by our studies with primary neuronal cultures from YAC128 HD mouse model [12,13]. It is generally assumed that many polyQ-expansion disorders share a common pathogenic mechanism [1-3]. Here we set out to investigate if abnormal Ca^{2+} signaling also plays a role in SCA3 pathogenesis. In a series of biochemcial and functional experiments we investigated interactions between ataxin-3 and $InsP_3R1$. We extended these findings to analysis of SCA3-YAC-84Q mouse model. Obtained results suggested that deranged neuronal Ca^{2+} signaling plays a significant role in SCA3 pathology.

Results

Mutant ataxin-3 specifically binds to and activates $InsP_3R1$ *in vitro*

To determine if $SCA3^{exp}$ behaves similar to Htt^{exp} and also binds to the $InsP_3R1$ carboxy-terminal region, we expressed EGFP-SCA3-19Q, EGFP-SCA3-77Q and EGFP-SCA3-127Q proteins [14] in HEK293 cells and performed a series of GST pull-down experiments with bacterially-expressed $InsP_3R1$ carboxy-terminal fragment GST-IC10 (aa F2627 - A2749 of rat $InsP_3R1$). The precipitated samples were analyzed by Western blotting with anti-GFP monoclonal antibodies. We found that GST-IC10, but not GST, specifically associated with GFP-SCA3-77Q and GFP-SCA3-127Q proteins (Fig 1A). Similar to Htt [10], association of ataxin-3 with IC10 fragment was dependent on polyQ expansion as wild type EGFP-SCA3-19Q protein did not bind to GST-IC10 (Fig 1A). In the next series of experiments we tested the association of full-length $InsP_3R1$ with ataxin-3. In these experiments we expressed full-length rat $InsP_3R1$ (RT1) in Sf9 cells by baculoviral infection and solubilized recombinant $InsP_3R1$ (RT1) in 1% CHAPS. The EGFP-SCA3-19Q, EGFP-SCA3-77Q and EGFP-SCA3-127Q proteins were transiently expressed in HEK293 cells as described above and solubilized in 1% CHAPS. The mixture of RT1 and ataxin-3 containing lysates was precipitated with anti-$InsP_3R1$ rabbit polyclonal antibodies (T443) [15] and analyzed by Western blotting with anti-GFP monoclonal antibodies. Preimmune sera (P/S) were used in control immunoprecipitation experiments. We found that full-length $InsP_3R1$ associated with EGFP-SCA3-77Q and EGFP-SCA3-127Q mutant proteins, but not with the wild type EGFP-SCA3-19Q protein (Fig 1B). Thus, association of full-length $InsP_3R1$ with ataxin-3 also depends on polyQ-expansion in ataxin-3 sequence.

To test functional effect of $SCA3^{exp}$ on $InsP_3R1$, we expressed full-length $InsP_3R1$ (RT1) in Sf9 cells by baculoviral infection, reconstituted recombinant $InsP_3R1$ in planar lipid bilayers and induced channel activity by addition of 100 nM $InsP_3$ to the *cis* chamber (Fig 1C). The SCA3-19Q and SCA3-77Q full-length proteins were expressed in bacteria as MBP (maltose-binding

protein) fusion proteins and purified by affinity chromatography followed by gel filtration. Obtained proteins were pure when analyzed by SDS-PAGE electrophoresis and Coomassie staining (data not shown). Addition of purified MBP or MBP-SCA3-19Q proteins had no effect on channel activity of $InsP_3R1$ in bilayers (Figs 1C, 1D). In contrast, addition of MBP-SCA3-77Q protein induced pronounced activation of $InsP_3R1$ (Fig 1E, 1F). In further experiments we generated baculoviruses encoding full-length SCA3-19Q and SCA3-77Q proteins. Microsomes prepared from Sf9 cells coinfected with RT1 and SCA3-19Q or SCA3-77Q baculoviruses were fused to planar lipid bilayers. In these experiments we found that $InsP_3R1$ co-expressed with SCA3-77Q are much more sensitive to activation by $InsP_3$ than the $InsP_3R1$ co-expressed with SCA3-19Q (Supplementary Fig 1). From these experiments we concluded that association of $SCA3^{exp}$ with $InsP_3R1$ increases apparent affinity of $InsP_3R1$ to activation by $InsP_3$, similar to our previous findings with Htt^{exp} [10].

Mutant ataxin-3 facilitates $InsP_3$-induced Ca^{2+} release in cells

To determine the functional effects of $SCA3^{exp}$ on $InsP_3R1$ in cells, we transfected cultured rat striatal medium spiny neurons (MSN) with SCA3-19Q, SCA3-77Q and SCA3-127Q expression plasmids. To identify transfected cells, the SCA3 plasmids were cotransfected with enhanced green fluorescent protein (EGFP)-expressing plasmid. To stimulate $InsP_3R1$-mediated Ca^{2+} release, we challenged Fura-2-loaded MSNs with 10 μM 3, 5-dihydroxyphenylglycine (DHPG), a specific mGluR1/5 receptor agonist. The local Ca^{2+} concentration in these experiments is estimated from the ratio of Fura-2 signals at 340 nm and 380 nm excitation wavelengths as shown by pseudocolor images (Fig. 2A). The transfected cells were identified by GFP imaging (Fig. 2A, first column) prior to collecting Ca^{2+} imaging data.

Ten micromolar DHPG corresponds to a threshold concentration for mGluR1/5 receptor activation in MSNs, and only a small response to DHPG application at this concentration was observed in control MSNs transfected with EGFP plasmid alone (Fig 2A, first row, Figs 2B and

2C) and in MSNs transfected with SCA3-19Q plasmid (Fig 2A, second row, Figs 2D and 2E). In contrast, significant response to 10 μM DHPG was observed in MSNs transfected with SCA3-77Q plasmid (Fig 2A, third row, Figs 2F and 2G). Even stronger response to DHPG was observed in MSNs transfected with SCA3-127Q plasmid (Fig 2A, fourth row, Figs 2H and 2I). On average, after the addition of 10 μM DHPG, the peak 340/380 ratios were significantly (p<0.01) higher than basal 340/380 ratios in SCA3-77Q and SCA3-127Q transfected neurons, but not in SCA3-19Q and EGFP-only transfected neurons (Fig 2K). Thus, we concluded that overexpression of $SCA3^{exp}$ mutant protein, but not of SCA3 wild type protein, sensitizes $InsP_3$-sensitive Ca^{2+} stores in cultured MSN.

To further investigate functional effects of $SCA3^{exp}$ on Ca^{2+} signaling in cells and to establish the relevance of our results for human disease, we performed a series of Fura-2 Ca^{2+} imaging experiments with primary human fibroblasts from from a healthy individual (hF) and a symptomatic SCA3 patient with 74Q expansion in ataxin-3 gene (hF-SCA3). We discovered that application of 300 nM bradykinin (BK), an agonist of $InsP_3$-coupled receptor, induced much larger Ca^{2+} responses in hF-SCA3 cells than in control hF cells (Supplementary Fig 2). From these experiments, we concluded that expression of mutant ataxin-3 proteins has potentiating effect on $InsP_3$R-mediated Ca^{2+} release in SCA3 patient fibroblasts, consistent with our analysis of Ca^{2+} signals in cultured rat MSN transfected with mutant $SCA3^{exp}$ (Fig 2).

Mutant ataxin-3 associates with $InsP_3$R1 *in vivo*

To establish a relevance of our findings for SCA3 pathogenesis *in vivo*, we focused on analysis of SCA3-YAC-84Q mouse model [16]. The SCA3-YAC-84Q mice used in these studies have been re-created by *in vitro* fertilization from a frozen sperm (see Methods for details). In the first series of experiments we assessed distribution of ataxin-3 protein in two brains from 12-month-old SCA3-YAC-84Q mice and two brains from 14-month-old SCA3-YAC-15Q mice [16]. We observed that the pattern of SCA3-84Q transgene expression and nuclear accumulation in

the aging SCA3-YAC-84Q mouse brains corresponded closely with the regions most severely affected in SCA3 patients, with abundant nuclear accumulation of ataxin-3 in pontine nuclei (Pn), substantia nigra (SN) and dentate nuclei (Lat) regions (Supplementary Fig 3). In contrast, nuclear accumulation of ataxin-3 was not detected in striatum (CPu), cortex and hippocampus (Supplementary Fig 3, data not shown), which are the brain regions relatively spared in MJD/SCA3 patients [5]. In SCA3-YAC-15Q mice ataxin-3 protein was expressed in a similar pattern but remained predominantly cytosolic and did not accumulate in the nucleus (Supplementary Fig 3).

To determine whether $SCA3^{exp}$ forms complex with $InsP_3R1$ *in vivo*, we performed a series of immunoprecipitation experiments with cortical lysates from wild type and SCA3-YAC-84Q mouse brains. Recombinant SCA3-19Q and SCA3-77Q proteins expressed in Sf9 cells were used as reference standards in these experiments (Fig 3). We found that anti-$InsP_3R1$ pAb (T443) precipitated SCA3-84Q from SCA3-YAC-84Q cortical lysates (Fig. 3, grey arrows). Consistent with *in vitro* binding experiments (Fig 1B), the association with $InsP_3R1$ was specific for mutant $SCA3^{exp}$, as endogenous mouse ataxin-3 was not precipitated by T443 pAb from wild type and SCA3-YAC-84Q mouse brains (Fig. 3, white arrows).

Dantrolene alleviates motor coordination deficits in SCA3-YAC-84Q mice

Biochemical and functional interactions between $SCA3^{exp}$ and $InsP_3R1$ (Figs 1-3, Supplementary Figs 1 and 2) suggested that deranged neuronal Ca^{2+} signaling may play a significant role in SCA3 pathogenesis. To test this hypothesis, we initiated a dantrolene trial in SCA3-YAC-84Q mice. Dantrolene is a skeletal muscle relaxant widely used in the clinic to treat malignant hyperthermia (MH) and muscle spasticity [17]. When used to treat MH, dantrolene acts by inhibiting excessive Ca^{2+} release from sarcoplasmic reticulum in skeletal muscles. In neuronal cells dantrolene has similar inhibitory effects on Ca^{2+} release from the endoplasmic reticulum [18]. The molecular target of dantrolene in muscle and neuronal cells is type 1

ryanodine receptor (RyanR1), an intracellular Ca^{2+} release channel. In experiments with cultured neuronal cells, dantrolene has been shown to have neuroprotective effect by inhibiting both cytosolic Ca^{2+} increase and neurotoxicity evoked by NMDA, glutamate, or potassium depolarization [18-22]. These results lead us to evaluate potential beneficial effects of dantrolene in SCA3-YAC-84Q mouse model.

In our studies 100 μg of dantrolene was resuspended in PBS and orally delivered to wild type (WT) and SCA3-YAC-84Q (SCA3) mice twice a week (Table 1, groups 2 and 4). Control groups of WT and SCA3 mice were fed with PBS alone at the same time (Table 1, groups 1 and 3). The effectiveness of drug delivery was determined by 2 months of "drug dosage" trial. We found that 30 min after feeding dantrolene concentration in blood plasma was 1081.25 ± 261.91 ng/ml and in brain it was 23.2 ± 4.2 ng/g (67 nM). Thus, we concluded that dantrolene accessed to the systemic circulation effectively from the gastrointestinal system, but penetrated blood brain barrier poorly, which is in agreement with the previous findings in the animal model of cerebral ischemia in gerbils [20].

The behavioral assessment of all 4 groups of mice was performed by using "beam walk" assay (see Methods for details). As in our previous studies [23], three kinds of beams (17 mm round, 11 mm round and 5 mm square) were used for testing. The "latency" and "number of footslips" were determined on each beam . When results were analyzed we found that control group of SCA3 mice (fed with PBS) exhibited a progressive impairment in beam-walking ability (longer beam traverse latencies and increased number of foot slips) with age and beam difficulty compared with control group of WT mice. The significant differences ($p < 0.05$) between beam performance of control SCA3 and control WT groups were observed at 10, 12 and 13.5 months of age on 17 mm round beam (Figs 4A, 4B); at 7.5, 10, 12 and 13.5 months of age on 11 mm round beam and 5 mm square beam (Figs. 4C, 4D, 4E, 4F). Feeding dantrolene to WT mice had no significant effect on balance beam performance of these mice (Fig. 4A-4F). However, feeding dantrolene to SCA3 mice improved their beam-walking performance, significantly

(p<0.05) shortening the latencies and decreasing the foot-slip numbers (Figs. 4A-4F). Significant differences ($p < 0.05$) of latency between SCA3 control group and dantrolene-fed SCA3 group were detected at 12 and 13.5 months of age on 17 round beam (Fig 4A); at 10, 12 and 13.5 months of age on 11 mm round beam and 5 mm square beam (Fig 4C, 4E). At 7.5, 10 and 12 month points, the number of foot slips of dantrolene-fed SCA3 mice on all 3 beams were almost identical to control WT mice (Figs 4B, 4D, 4F). We noticed that following dantrolene withdrawal, the perfomance of both WT and SCA3 groups of mice was impaired, with increased latencies and elevated numbers of footslips (Figs 4A-4F). This phenomenon is most likely to be due to removal of the sedative effect of dantrolene, which resulted in anxiousness of the mice. In spite of this “withdrawal effect” dantrolene-fed SCA3 mice still performed better than control SCA3 mice in most tasks at 13.5 months time point (Figs 4A-4F).

While conducting beam-walking assays, we observed that some aging mice exhibited periods of "crawling behavior" (defined as prolonged contact between the thorax and abdomen of the mice and beam surface, with the mice using forelimbs to drag themselves along the beam). Two mice in SCA3 control group crawled on 11 mm round and 5 mm square beams at 10 months time point, three mice in SCA3 control group crawled on 11 mm round beam and 5 mm square beam at 12 and 13.5 months of age, and two mice in SCA3 dantrolene-fed group crawled on 5 mm square beam at 12 and 13.5 months of age. Furthermore, one mouse in SCA3 control group fell off 5 mm square beam when tested at 12 and 13.5 months time points (Figs 4E, 4F). In contrast, none of the mice in WT groups exhibited crawling behavior or fell off the beams at any age tested. The incidence of crawling behavior was consistent with a general performance of these mice in balance beam assay, with SCA3 control group performing the worst, dantrolene-fed SCA3 group performing better and all the wild type mice traversing the beams without crawling.

At the conclusion of beam walking behavioral experiments (13.5 months of age), we assessed gait abnormalities in the four groups of mice by using footprint pattern analysis (Fig. 4G). The footprint patterns were assessed quantitatively by the measurements of stride length and front/hind footprint overlap as we previously described [23] . We found that the stride length of SCA3 control mice was very significantly ($p<0.001$) shorter than WT control littermates (Figs. 4G, 4H). Dantrolene feeding significantly ($p<0.01$) increased the stride length of SCA3 mice, but had no obvious effects on stride length of WT mice (Figs. 4G, 4H). We further found that front/hind footprint overlap was significantly higher in SCA3 control group than in WT control group (Fig 4I). In contrast to stride length measure, footprint overlap deficit was not rescued by feeding dantrolene to SCA3 mice (Fig 4I).

Dantrolene protects against neuronal loss in SCA3-YAC-84Q mice

To further evaluate potential neuroprotective effects of dantrolene, at the conclusion of behavioral analysis (13.5 months time point) the brains from all four groups of experimental mice were removed from skull and weighed after transcardial perfusion. We found that the brains of control SCA3 mice (fed with PBS) weighted significantly less ($p < 0.01$) than the brains of control WT mice group (Fig 5A, Table 1). Feeding dantrolene to WT mice had no significant effect on brain weight of these mice (Fig 5A, Table 1), while the brain weight of SCA3 mice fed with dantrolene was higher than the brain weight of control SCA3 mice (Fig 5A, Table 1), although the difference did not reach a level of statistical significance.

In order to obtain quantitative information about neuronal loss in the experimental mice, we performed stereological analysis of these brains. Our analysis was focused on pontine nuclei (Pn) and substantia nigra (SN) regions, both of which severely affected in SCA3 patients [5]. Our own experiements confirmed abundant accumulation of SCA3-84Q transgene in neurons from Pn and SN regions in brains form aging SCA3-YAC-84Q mice (SupFig 3). For

stereological analysis NeuN-positive neurons in Pn and TH-positive neurons in SN were counted blindly with respect to the nature of slices (genotype and drug treatment). We focused on TH-positive neurons in SN as dopaminergic neurons are most severely affected in SCA3 patients [5] and our own analysis demonstrated that SCA3-84Q transgene is primarily expressed in SN dopaminergic neurons of SCA3-YAC-84Q mice (data not shown). By stereological analysis we determined that control SCA3 mice (fed with PBS) showed significant neuronal loss in Pn ($p < 0.05$) and SN ($p < 0.01$) when compared with control WT mice (Figs. 5B and 5C, Table 1). We further found that feeding of dantrolene had no significant effect on Pn and SN neuronal counts in WT mice but significantly increased Pn and SN neuronal counts ($p < 0.01$) in SCA3 mice (Figs. 5B and 5C, Table 1). Our results indicated that feeding with dantrolene protected most Pn and SN neurons from cell death in brains of aging SCA3 mice (Figs. 5B and 5C, Table 1).

Discussion

The causes of neurodegeneration in SCA3 and other polyQ-expansion disorders are poorly understood. Similar to other polyQ-expansion disorders, mutant ataxin-3 forms nuclear agreggates, and formation of these aggregates have been proposed to be toxic to the affected neurons [24,25]. The nuclear toxicity of ataxin-3 has been supported by recent genetic experiments with transgenic mouse model of SCA3 [26]. Consistent with the presence of Josephin domain and ubiquitin-interactions motifs, ataxin-3 binds polyubiquitylated proteins and displays deubiquitylating activity *in vitro* [27,28]. In agreement with defects in ubiqutin-proteasomal pathway, impaired proteasomal function has been implicated in SCA3 pathogenesis [29]. Results of our studies indicate that in addition to forming “toxic aggregates” and causing “proteasomal deficiency” mutant ataxin-3 is also able to destabilize neuronal Ca^{2+} signaling. We found that mutant ataxin-3 directly binds to the $InsP_3R1$ (Figs 1A, 1B, 3) and increases

sensitivity of $InsP_3R1$ to activation by $InsP_3$ in functional assays (Figs 1C-1F, 2 and Supplementary Figs 1 and 2). The mechanism of $SCA3^{exp}$ effects on $InsP_3R1$ and Ca^{2+} signaling in our experiments are identical to actions of Htt^{exp} which we described previously [10]. Studies of Htt^{exp} and Ca^{2+} signaling led us to propose "Ca^{2+} hypothesis of HD [11], and idea supported by our studies with primary neuronal cultures from YAC128 HD mouse model [12,13]. Biochemical and functional interactions between mutant ataxin-3 and $InsP_3R1$ (Figs 1 – 3, Supplementary Figs 1 and 2) suggested that deranged neuronal Ca^{2+} signaling may also play a significant role in SCA3 pathogenesis. To test this hypothesis we evaluated the effects of dantrolene, a clinically relevant stabilizer of intracellular Ca^{2+} signaling and inhibitor of ryanodine receptor, on the phenotype of SCA3-YAC-84Q transgenic mouse. We found that feeding SCA3-YAC-84Q mice with dantrolene improved their motor performance (Fig 4) and prevented neuronal cells loss in pontine nuclei and substantia nigra regions (Fig 5 and Table 1). Our results indicate that deranged neuronal Ca^{2+} signaling may play an important role in SCA3 pathology and that Ca^{2+} signaling stabilizers such as dantrolene may be considered as potential therapeutic drugs for treatment of SCA3 patients.

MATERIALS and METHODS

SCA3 mouse colonies. Generation of SCA3-YAC-15Q and SCA3-YAC-84Q mice have been previously described [16]. For our studies SCA3-YAC-84Q mouse was recreated by IVF using C57BL/6 mouse strain egg and SCA3-YAC-84Q mouse frozen sperm.

In vitro binding experiments

EGFP-SCA3-19Q, EGFP-SCA3-77Q and EGFP-SCA3-127Q expression plasmids have been previously described [14]. GST-IC10 expression plasmid (aa F2627 - A2749 of rat $InsP_3R1$) has been previously described [10]. GST and GST-IC10 proteins were expressed in the BL21 *E. coli* strain and purified on glutathione-agarose beads. EGFP-SCA3-19Q/77Q/127Q proteins were expressed in HEK293 cells by calcium-phosphate transfection. 48 hr after transfection, HEK293 cells were collected with ice-cold PBS and solubilized for 30 min at 4°C in extraction buffer A (1% CHAPS, 137 mM NaCl, 2.7 mM KCl, 4.3 mM Na_2HPO_4, 1.4 mM KH_2PO_4 [pH 7.2], 5 mM EDTA, 5 mM EGTA, and protease inhibitors). Extracts were clarified by centrifugation for 20 min at 100,000 × g and incubated for 1 hr at 4°C with GST or GST-IC10 proteins. Beads were washed three times with extraction buffer A. Attached proteins were analyzed by Western blotting with anti-GFP monoclonal antibodies.

Full-length rat $InsP_3R1$ (RT1)-encoding baculoviruses were previously described [30]. The EGFP-SCA3-19Q, EGFP-SCA3-77Q and EGFP-SCA3-127Q proteins were transiently expressed in HEK293 cells as described above and solubilized in 1% CHAPS. The mixture of RT1 and ataxin-3 containing lysates was precipitated with anti-$InsP_3R1$ polyclonal antibody (T443) [15] attached to protein A-Sepharose beads and analyzed by Western blotting with anti-GFP monoclonal antibodies. Preimmune sera (P/S) were used in control immunoprecipitation experiments.

Planar Lipid Bilayer Experiments. Single-channel recordings of recombinant $InsP_3R1$ (RT1) were performed as previously described [10] at 0 mV transmembrane potential using 50 mM Ba^{2+} (*trans*) as a charge carrier. The *cis* (cytosolic) chamber contained 110 mM Tris dissolved in HEPES (pH 7.35), 0.5 mM Na_2ATP, pCa 6.7 (0.2 mM EGTA + 0.14 mM $CaCl_2$) [31]. $InsP_3R1$ were activated by addition of 100 nM $InsP_3$ (Alexis) to the *cis* chamber as indicated in the text. Coding sequences of SCA3-19Q/77Q proteins were subcloned into pMAL2 bacterial expression vector (New England Biolabs). MBP, MBP-SCA3-19Q, MBP-SCA3-77Q proteins were expressed in *BL21 E. coli*, purified on amylose resin (New England Biolabs) followed by gel filtration on Sephadex-10 column (AKTA FPLC, Amersham-Pharmacia). The proteins were dialyzed overnight against *cis* recording buffer (110 mM Tris/HEPES [pH 7.35]), and added in 1 µl volume (0.3 mg/ml protein with addition of 0.02 mM ruthenium red) directly to the *cis* side of the bilayer containing $InsP_3R1$ without stirring. Exposure of $InsP_3R1$ to the test proteins was terminated 2–3 min after addition by stirring the *cis* chamber for 30 s (1:3000 dilution of test protein stocks). The $InsP_3R1$ single-channel currents were amplified (Warner OC-725), filtered at 1 kHz by a low-pass eight-pole Bessel filter, digitized at 5 kHz (Digidata 1200, Axon Instruments), and stored on computer hard drive and recordable optical discs. For off-line computer analysis (pClamp 6, Axon Instruments), currents were filtered digitally at 500 Hz. For presentation of the current traces, data were filtered at 200 Hz.

Ca^{2+} Imaging Experiments. The rat medium spiny neuronal (MSN) cultures on poly-D-lysine (Sigma) coated 12 mm round glass coverslips were established as previously described [10]. The 5 µM of cytosine arabinoside (AraC, Sigma) was added at 2–4 DIV to inhibit glial cell growth. SCA3-19Q, SCA3-77Q and SCA3-130Q expression plasmids in pcDNA3 vector were generated by subcloning from EGFP-SCA3 plasmids described above. At 20 DIV the MSN cultures were transfected by the calcium-phosphate method with EGFP-C3 plasmid (Clontech) or a 1:3 mixture of EGFP: SCA3 expression plasmids as indicated in the text. 48 hr after transfection,

the MSN neurons were loaded with 5 μM Fura-2-AM (Molecular Probes) in artificial cerebrospinal fluid (ACSF) (140 mM NaCl, 5 mM KCl, 1 mM $MgCl_2$, 2 mM $CaCl_2$, 10 mM HEPES [pH 7.3]) for 45 min at 37°C. For imaging experiments the coverslips were mounted onto a recording/perfusion chamber (RC-26G, Warner Instrument) maintained at 37°C (PH1, Warner Instrument), positioned on the movable stage of an Olympus IX-70 inverted microscope, and perfused with ACSF media by gravity flow. Following GFP imaging, the coverslip was washed extensively with Ca^{2+}-free ACSF (omitted $CaCl_2$ from ACSF and supplemented with 100 μM EGTA). In Ca^{2+} imaging experiments the MSN cells were intermittently excited by 340 nm and 380 nm UV light (DeltaRAM illuminator, PTI) using a Fura-2 dichroic filter cube (Chroma Technologies) and 60× UV-grade oil-immersed objective (Olympus). The emitted light was collected by an IC-300 camera (PTI), and the images were digitized by ImageMaster Pro software (PTI). Baseline (6 min) measurements were obtained prior to bath application of 10 μM 3, 5-DHPG (Tocris) dissolved in Ca^{2+}-free ACSF. The DHPG solutions were prewarmed to 37°C before application to MSNs. Images at 340 and 380 nm excitation wavelengths were captured every 5 s and shown as 340/380 image ratios at time points as indicated. Background fluorescence was determined according to manufacturer's (PTI) recommendations and subtracted.

Brain immunoprecipitations. Brains of wild type and SCA3-YAC-84Q mice were collected out of skull. After taking away cerebella, the brain samples were homogenized and solubilized at 4ºC for 2 hr in extraction buffer A (1% CHAPS, 137mM NaCl, 2.7mM KCl, 4.3mM Na_2HPO_4, 1.4mM KH_2PO_4 [pH7.2], 5mM EDTA, 5mM EGTA and protease inhibitors). The homogenates were cleared by 30 min centrifugation at 50,000 rpm in TL-100 and incubated with anti-$InsPR_3$ polyclonal antibodies (T443) attached to protein-A Sepharose CL-4B beads (Amersham Biosciences) at 4ºC for 3 hr. The resulted beads were washed with extraction buffer A and analyzed by Western blotting with anti-Ataxin-3 monoclonal antibody (Chemicon, MAB5360).

Drug delivery in mice. Dantrolene was delivered to mice by an approach that we used previously in tetrabenzine trial in YAC128-HD mice [23]. Briefly, groups of wild type and SCA3-YAC-84Q mice were fed with 100 μg dantrolene suspended in 50 μl PBS with 2% corn flour resulting in the dosage 5 mg/kg. The control groups were fed with 2% corn flour in PBS. All mice were fed orally twice a week from 2 to 12 months old. In order to decide the concentration of dantrolene in mouse brains, 5 wild type mice of 2 months old were fed with dantrolene for 2 months with the same dosage (5 mg/kg) and anesthetized 30 min after the last dantrolene feeding. The blood samples of 5 mice were harvested into a tube containing 50 μl ACD solution (2.2 g sodium citrate; 0.8 g citric acid, monohydrate; 2.24 g glucose, anhydrous dissolved in dH_2O to the final volume 100ml). After spinning the blood samples at 4ºC, 10,000 rpm for 10 min, plasma was isolated and transferred to -80 ºC immediately. The brains were collected at the same time and snap frozen in liquid nitrogen. The plasma and brain samples from each mouse were numbered and shipped on dry ice to the core facility of the department of Biochemistry in UT Southwestern for analysis by HPLC.

Motor coordination assessments in mice. The motor coordination experiments were performed as previously described [23]. The "beam walking" assay was carried out using a home-made experimental setup. The 17 mm round plastic beam, 11 mm round plastic beam, and 5 mm square wood beam were used in our studies. At each time point, the mice were trained on beams for 3 consecutive days (4 trials /d) to traverse the beam to the enclosed box. Once the stable baseline of performance was obtained, the mice were tested in three consecutive trials on 17 and 11 mm round plastic beams and 5 mm square wood beam, in each case progressing from the widest to the narrowest beam. The latency to traverse the middle 80 cm of each beam and the number of times the hind feet slipped off each beam were recorded for each trial. For each measure, the mean scores of the three trials for each beam were used in the analysis.

For the footprint test, the forepaws and hindpaws of the mice were coated with purple and green nontoxic paints, respectively. The mice were trained to walk along a 50-cm-long, 10-cm-wide, paper-covered runway (with 10-cm-high walls) into an enclosed box. All the mice were given 3 runs/d for 3 consecutive days. A fresh sheet of white paper was placed on the floor of the runway for each run. The footprint patterns were assessed quantitatively by the measurements of stride length and front/hindpaw overlap as we described previously [23].

Neuropathological assessments in mice. The neuropathological assessments were performed as previously described [23]. After all the behavioral testings (13.5 months time point), the mice were terminally anesthetized by pentobarbital with the dosage of 60 mg/kg and perfused transcardially with 20 ml of 0.9% saline followed by 100 ml of fixative (4% paraformaldehyde in 0.1 M PBS, pH 7.4). All brains were removed from skull, weighed and transferred to postfixative (4% paraformaldehyde in 0.1 M PBS, pH 7.4). After postfixation overnight at 4°C, the brains were infiltrated in 20–30% (w/v) sucrose in PBS at 4°C for 24-48 hr until falling to the bottom. The brains were frozen on dry ice and cut to 30-μm-thick coronal sections using a Leica (Bannockburn, IL) SM2000R sliding microtome. The coronal slices spaced 90 μm apart throughout the pontine (Pn) were stained with anti-NeuN monoclonal antibody (1:1000 dilution; Millipore, Billerica, MA). The coronal sections spaced 120 μm apart throughout the substantia nigra (SN) were stained with anti- tyrosine hydroxylase (TH) monoclonal antibody (1:400 dilution; Millipore, Billerica, MA). Biotinylated anti-mouse IgG reagent was used in all the staining as the secondary antibodies (1:250 dilution; Vector Laboratories, Burlington, Ontario, Canada) (M.O.M kit). Signal was amplified with an ABC Elite kit (Vector Laboratories) and detected with diaminobenzidine (Vector Laboratories). All quantitative stereological analyses were performed blindly with respect to the nature of slices (genotype and drug feeding) using Stereoinvestigator setup and software (MicroBrightField, Williston, VT). For neuronal counting in Pn, the grid size was set to 250 x 200 μm and the

counting frame size was 40 x 40 µm. For neuronal counting in SN, the grid size was set to 130 x 100 µm and the counting frame size was 50 x 50 µm. The average slice thickness after histological processing was determined to be 22 µm.

Statistical data analysis. For comparison between two groups, Student's unpaired *t* test was used to statistically analyze data.

Figure 1. Biochemical and functional interactions between ataxin-3 and $InsP_3R1$.

(A) GST/GST-IC10 pull-down experiments of EGFP-SCA3-19Q/77Q/127Q proteins from HEK293 cell extracts.

(B) Immunoprecipitation of EGFP-SCA3/19Q/77Q/127Q from HEK293 cell lysates with full-length $InsP_3R1$ (RT1) expressed in Sf9 cells. Anti-$InsP_3R1$ polyclonal antibodies (T443) and corresponding control preimmune sera (P/S) were used for precipitation.

The precipitated fractions on panels A and B were analyzed by Western blotting with anti-GFP monoclonal antibodies.

(C, E) Effects of MBP, MBP-SCA3-19Q and MBP-SCA3-77Q on the activity of recombinant $InsP_3R1$ in planar lipid bilayers at 100 nM $InsP_3$. Each current trace corresponds to 10 s (2 s for expanded traces) of current recording for the same experiment.

(D, F) The average open probability (P_o) of $InsP_3R1$ at 100 nM of $InsP_3$ in the presence of MBP, MBP-SCA3-19Q and MBP-SCA3-77Q. The average P_o was calculated for a 5 s window of time and plotted for the duration of an experiment. The times of $InsP_3$, MBP, MBP-SCA3-19Q and MBP-SCA3-77Q additions are shown above the P_o plot. Data from the same experiment are shown on (C, D) and (E, F). Similar results were obtained in at least three independent experiments with MBP-SCA3-19Q and MBP-SCA3-77Q.

Figure 2. Effects of ataxin-3 on DHPG-induced Ca^{2+} release in MSN.

(A) Representative images showing Fura-2 340/380 ratios in transfected rat MSNs. The pseudocolor calibration scale for 340/380 ratios is shown on the right. Ratio recordings are shown for 10 μM DHPG-induced Ca^{2+} transients in MSNs transfected with EGFP (first row), EGFP + SCA3-19Q (second row), EGFP + SCA3-77Q (third row), and EGFP + SCA3-127Q (fourth row). The recordings were performed in Ca^{2+}-free ACSF containing 100 μM EGTA. GFP images (1st column) were captured before Ca^{2+} imaging to identify transfected cells. 340/380 ratio images are shown for MSN neurons 1 min before (2^{nd} column), and 8 s, 30 s, 1 min, 2 min, and 3 min after application of 10 μM DHPG as indicated. We used SCA3: EGFP plasmids at a 3:1 ratio during transfections, which probably resulted in the expression of SCA3 in some GFP-negative MSNs. The GFP-negative cells that respond to 10 μM DHPG in the third and fourth row (triangle arrow) are interpreted to be the neurons transfected with SCA3-77Q or SCA3-127Q plasmid alone. Only GFP-positive MSNs were considered for quantitative analyses.

(B, D, F, H) Basal and peak 340/380 ratios are shown for individual MSN neurons transfected with EGFP (B), EGFP+SCA3-19Q (D), EGFP+SCA3-77Q (F), EGFP+SCA3-127Q (H). The experiments were performed as described on panel A. The basal ratios were determined 1 min prior to DHPG application (−1 min). The peak ratios were measured from maximal signals observed within 30 s after DHPG application. 340/380 ratio traces for representative cells (marked *) are shown in (C), (E), (G) and (I). Time of DHPG application is shown. Similar results were obtained in four independent transfections.

(K) Summary of MSN Ca^{2+} imaging experiments with SCA3 constructs. Average basal and DHPG-evoked peak 340/380 ratios from four independent transfections are shown as mean ± SEM (n = number of cells). The peak ratios in MSNs transfected with EGFP + SCA3-77Q and EGFP + SCA3-127Q are significantly (***$p < 0.01$, paired t test) higher than the basal ratios in the same cells.

Figure 3. Association of ataxin-3 with $InsP_3R1$ *in vivo* .

Cortical lysates from WT and SCA3-YAC-84Q mouse were precipitated by anti-$InsP_3R1$ pAb (T443) and analyzed by Western blotting with anti-ataxin-3 mAb. Lysates from Sf9 cells infected with SCA3-19Q (white arrow) and SCA3-77Q (grey arrow) recombinant baculoviruses were used as reference standards. Endogenous mouse ataxin-3 (white arrow) was detected by anti-ataxin3 (atx3) mAb in cortical lysates from the wild type and SCA3-YAC-84Q mice. SCA3-84Q transgene (grey arrow) were detected in cortical lysates from the SCA3-YAC-84Q mouse. Anti-$InsP_3R1$ pAb (T443) precipitated SCA3-84Q (grey arrow), but not the endogenous ataxin-3. Preimmune serum (P/S) was used as a negative control for T443 immunoprecipitation experiments.

Figure 4. Motor coordination performance of WT and SCA3 mice in dantrolene trial.

(A-F) Beam walk assay. The average time to cross the beam (A, C, E) and the average number of foot slips on the beam (B, D, F) are shown for beam walking experiments performed with 17 mm round plastic beam (A, B), 11 mm round plastic beam (C, D), and 5 mm square wood beam (E, F). The data for WT control mice (open black circles), SCA3 control mice (filled black circles), WT mice fed with dantrolene (open red circles), SCA3 mice fed with dantrolene (filled red circles) are shown as mean ± SEM (for the number of mice in each group, see Table 1) at 2, 4, 7.5, 10, 12 and 13.5 month (washout) time points. While counting the footslips of the mice with "crawling behavior", we considered every step as one footslip. *** $p < 0.05$, significant differences between control SCA3 group and dantrolene-fed SCA3 group. "1F" on panels E and F means one mouse failed the test.

(G-I) Gait analysis. (G) The footprint patterns of 13.5-month-old SCA3 and WT mice. The footprints for control and dantrolene groups are shown for both WT and SCA3 mice.

(H) Stride lengths of WT and SCA3 ice in dantrolene trial are shown as mean ± SEM (for the number of mice in each group, see Table 1). Feeding dantrolene to SCA3 mice significantly ($p<0.001$) increased the stride lengths.

(I) Front/hind footprint overlaps of WT and SCA3 mice in dantrolene trial are presented as mean ± SEM. Feeding dantrolene to SCA3 mice had no effect on front/hind paw overlaps.

Figure 5. Neuroanatomical analysis of WT and SCA3 mice in dantrolene trial.

(A) Average brain weight of 13.5-month-old WT and SCA3 mice. The brain weight of control SCA3 mice is significantly reduced compared with control WT group ($p < 0.01$). The brain weight of SCA3 mice fed with dantrolene is higher than control SCA3 mice, but the difference is not statistically significant.

(B) Average pontine nuclei (Pn) neuronal counts of 13.5-month-old WT and SCA3 mice are shown as mean ± SEM (for the number of mice in each group, see Table 1) . Control SCA3 mice showed significant Pn neuronal loss (***$p < 0.05$) compared with control WT mice. SCA3 mice fed with dantrolene exhibited significantly (***$p < 0.01$) increased Pn neuronal counts compared with control SCA3 mice.

(C) Average substantia nigra (SN) neuronal counts of TH-positive neurons from 13.5-month-old WT and SCA3 mice are shown as mean ± SEM (for the number of mice in each group, see Table 1). The SN-TH neuronal number in control SCA3 mice is significantly lower (***$p < 0.01$) than in control WT mice. In SCA3 mice fed with dantrolene, the SN-TH neuronal counts are significantly (***$p < 0.01$) increased when compared to control SCA3 mice.

References

1. Gusella, J.F. & MacDonald, M.E. Molecular genetics: unmasking polyglutamine triggers in neurodegenerative disease. *Nat Rev Neurosci* 1, 109-115 (2000).

2. Zoghbi, H.Y. & Orr, H.T. Glutamine repeats and neurodegeneration. *Annu Rev Neurosci* 23, 217-247 (2000).

3. Cummings, C.J. & Zoghbi, H.Y. Trinucleotide repeats: mechanisms and pathophysiology. *Annu Rev Genomics Hum Genet* 1, 281-328 (2000).

4. Coutinho, P. & Andrade, C. Autosomal dominant system degeneration in Portuguese families of the Azores Islands. A new genetic disorder involving cerebellar, pyramidal, extrapyramidal and spinal cord motor functions. *Neurology* 28, 703-709 (1978).

5. Stevanin, G., Durr, A. & Brice, A. Clinical and molecular advances in autosomal dominant cerebellar ataxias: from genotype to phenotype and physiopathology. *Eur J Hum Genet* 8, 4-18 (2000).

6. Kawaguchi, Y.*, et al.* CAG expansions in a novel gene for Machado-Joseph disease at chromosome 14q32.1. *Nat Genet* 8, 221-228 (1994).

7. Paulson, H.L.*, et al.* Machado-Joseph disease gene product is a cytoplasmic protein widely expressed in brain. *Ann Neurol* 41, 453-462 (1997).

8. Scheel, H., Tomiuk, S. & Hofmann, K. Elucidation of ataxin-3 and ataxin-7 function by integrative bioinformatics. *Hum Mol Genet* 12, 2845-2852 (2003).

9. Nicastro, G.*, et al.* The solution structure of the Josephin domain of ataxin-3: Structural determinants for molecular recognition. *Proc Natl Acad Sci U S A* 102, 10493-10498 (2005).

10. Tang, T.-S.*, et al.* Huntingtin and huntingtin-associated protein 1 influence neuronal calcium signaling mediated by inositol-(1,4,5) triphosphate receptor type 1. *Neuron* 39, 227-239 (2003).

11. Bezprozvanny, I. & Hayden, M.R. Deranged neuronal calcium signaling and Huntington disease. *Biochem Biophys Res Commun* 322, 1310-1317 (2004).

12. Tang, T.-S.*, et al.* Disturbed Ca2+ signaling and apoptosis of medium spiny neurons in Huntington's disease. *Proc Natl Acad Sci U S A* 102, 2602-2607 (2005).

13. Wu, J., Tang, T.-S. & Bezprozvanny, I. Evaluation of clinically-relevant glutamate pathway inhibitors in in vitro model of Huntington's disease. *Neurosci Lett* 407, 219-223 (2006).

14. Wang, G., Sawai, N., Kotliarova, S., Kanazawa, I. & Nukina, N. Ataxin-3, the MJD1 gene product, interacts with the two human homologs of yeast DNA repair protein RAD23, HHR23A and HHR23B. *Hum Mol Genet* 9, 1795-1803 (2000).

15. Kaznacheyeva, E., Lupu, V.D. & Bezprozvanny, I. Single-channel properties of inositol (1,4,5)-trisphosphate receptor heterologously expressed in HEK-293 cells. *J Gen Physiol* 111, 847-856 (1998).

16. Cemal, C.K.*, et al.* YAC transgenic mice carrying pathological alleles of the MJD1 locus exhibit a mild and slowly progressive cerebellar deficit. *Hum Mol Genet* 11, 1075-1094 (2002).

17. Krause, T., Gerbershagen, M.U., Fiege, M., Weisshorn, R. & Wappler, F. Dantrolene--a review of its pharmacology, therapeutic use and new developments. *Anaesthesia* 59, 364-373 (2004).

18. Makarewicz, D., Zieminska, E. & Lazarewicz, J.W. Dantrolene inhibits NMDA-induced 45Ca uptake in cultured cerebellar granule neurons. *Neurochem Int* 43, 273-278 (2003).

19. Frandsen, A. & Schousboe, A. Dantrolene prevents glutamate cytotoxicity and Ca2+ release from intracellular stores in cultured cerebral cortical neurons. *J Neurochem* 56, 1075-1078 (1991).

20. Wei, H. & Perry, D.C. Dantrolene is cytoprotective in two models of neuronal cell death. *J Neurochem* 67, 2390-2398 (1996).

21. Niebauer, M. & Gruenthal, M. Neuroprotective effects of early vs. late administration of dantrolene in experimental status epilepticus. *Neuropharmacology* 38, 1343-1348 (1999).

22. Guo, Q.*, et al.* Increased vulnerability of hippocampal neurons to excitotoxic necrosis in presenilin-1 mutant knock-in mice. *Nat Med* 5, 101-106 (1999).

23. Tang, T.S., Chen, X., Liu, J. & Bezprozvanny, I. Dopaminergic signaling and striatal neurodegeneration in Huntington's disease. *J Neurosci* 27, 7899-7910 (2007).

24. Paulson, H.L.*, et al.* Intranuclear inclusions of expanded polyglutamine protein in spinocerebellar ataxia type 3. *Neuron* 19, 333-344 (1997).

25. Perez, M.K., Paulson, H.L. & Pittman, R.N. Ataxin-3 with an altered conformation that exposes the polyglutamine domain is associated with the nuclear matrix. *Hum Mol Genet* 8, 2377-2385 (1999).

26. Bichelmeier, U.*, et al.* Nuclear localization of ataxin-3 is required for the manifestation of symptoms in SCA3: in vivo evidence. *J Neurosci* 27, 7418-7428 (2007).

27. Burnett, B., Li, F. & Pittman, R.N. The polyglutamine neurodegenerative protein ataxin-3 binds polyubiquitylated proteins and has ubiquitin protease activity. *Hum Mol Genet* 12, 3195-3205 (2003).

28. Burnett, B.G. & Pittman, R.N. The polyglutamine neurodegenerative protein ataxin 3 regulates aggresome formation. *Proc Natl Acad Sci U S A* 102, 4330-4335 (2005).

29. Chai, Y., Koppenhafer, S.L., Shoesmith, S.J., Perez, M.K. & Paulson, H.L. Evidence for proteasome involvement in polyglutamine disease: localization to nuclear inclusions in SCA3/MJD and suppression of polyglutamine aggregation in vitro. *Hum Mol Genet* 8, 673-682 (1999).

30. Tu, H.*, et al.* Functional characterization of the type 1 inositol 1,4,5-trisphosphate receptor coupling domain SII(+/-) splice variants and the *opisthotonos* mutant form. *Biophys J* 82, 1995-2004 (2002).

31. Bezprozvanny, I., Watras, J. & Ehrlich, B.E. Bell-shaped calcium-response curves of Ins(1,4,5)P_3- and calcium-gated channels from endoplasmic reticulum of cerebellum. *Nature* 351, 751-754 (1991).

Table 1. Dantrolne trial in SCA3-YAC-84Q mice.

Four groups of mice were tested in our experiments. At 2 months of age, WT and 84Q mice were divided into two groups each and drug treatment was initiated. The group number, group name, number and genotype of mice in each group, and dose of single drug treatment (twice/week) are shown for each group. Also shown is the estimated drug dosage in mg/kg body weight. The results of neuroanatomical analysis are shown for each group. The average brain weight, Pn neuronal counts and SN-TH neuronal counts are shown as mean ± SEM (n = number of mice in each group).

Group number	Group name	Number of female mice	Mouse genotype	Single dose (2/wk) (50µl)	Drug dosage (mg/kg/3 days)	Brain weight (g)	Pn counts	SN-TH counts
1	WT-Ctrl	10	WT	50 µl PBS	PBS	0.500 ± 0.008	43368 ± 1811	11026 ± 284
2	WT-Dan	7	WT	100 µg Dantrolene	5 mg Dantrolene	0.501 ± 0.004	43659 ±2203	11202 ± 254
3	SCA3-Ctrl	8	SCA3-YAC-84Q	50 µl PBS	PBS	0.451 ± 0.007	37021 ± 1000	9384 ± 250
4	SCA3-Dan	10	SCA3-YAC-84Q	100 µg Dantrolene	5 mg Dantrolene	0.470 ± 0.007	43642 ± 1725	10699 ± 239

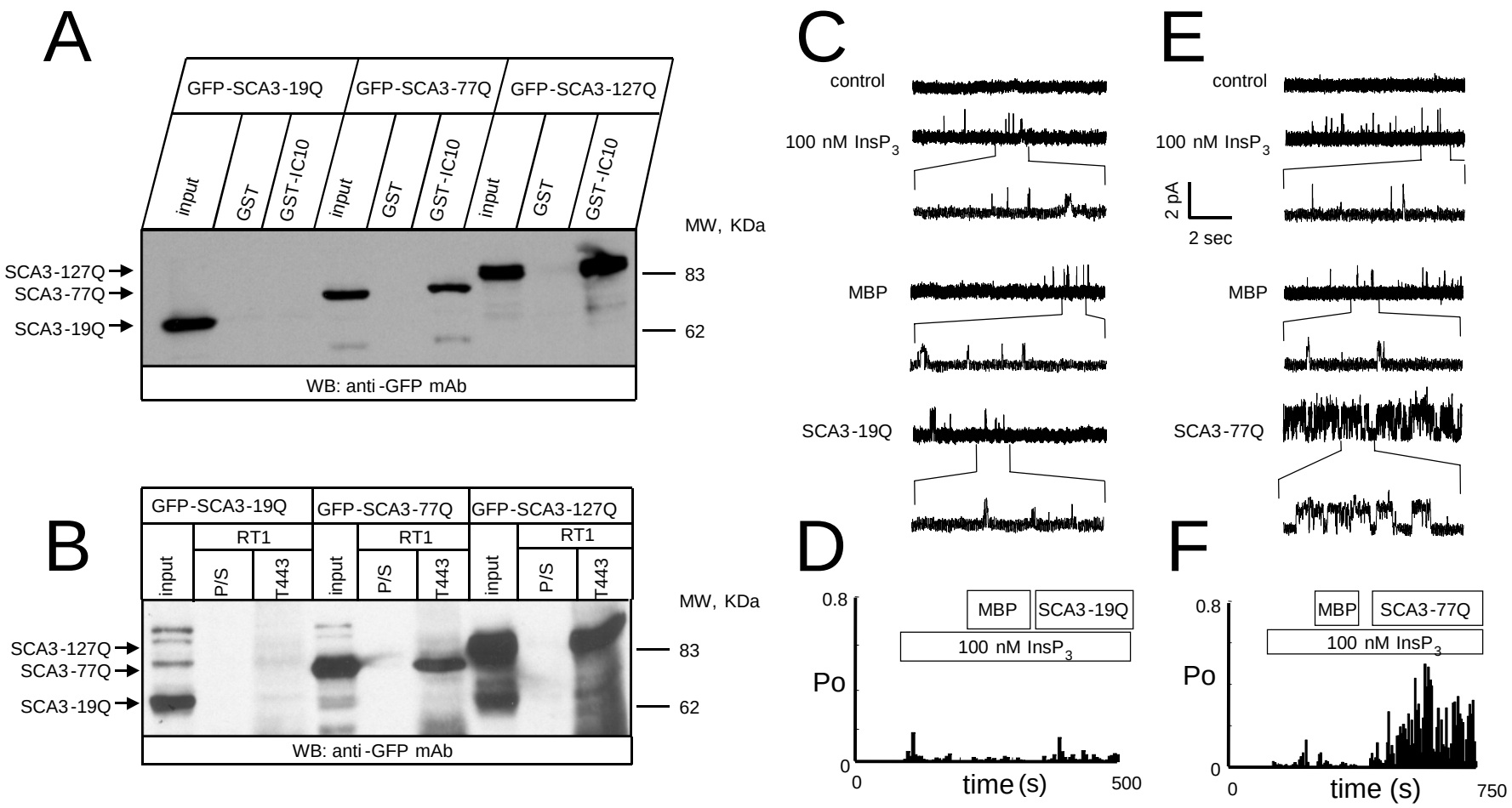
A
GFP-SCA3-19Q
GFP-SCA3-77Q
GFP-SCA3-127Q
input
GST
GST-IC10
MW, KDa
SCA3-127Q
SCA3-77Q
SCA3-19Q
83
62
WB: anti-GFP mAb
B
RT1
P/S
T443
C
control
100 nM InsP3
MBP
SCA3-19Q
D
Po
time (s)
E
2 pA
2 sec
SCA3-77Q
F

Fig 1

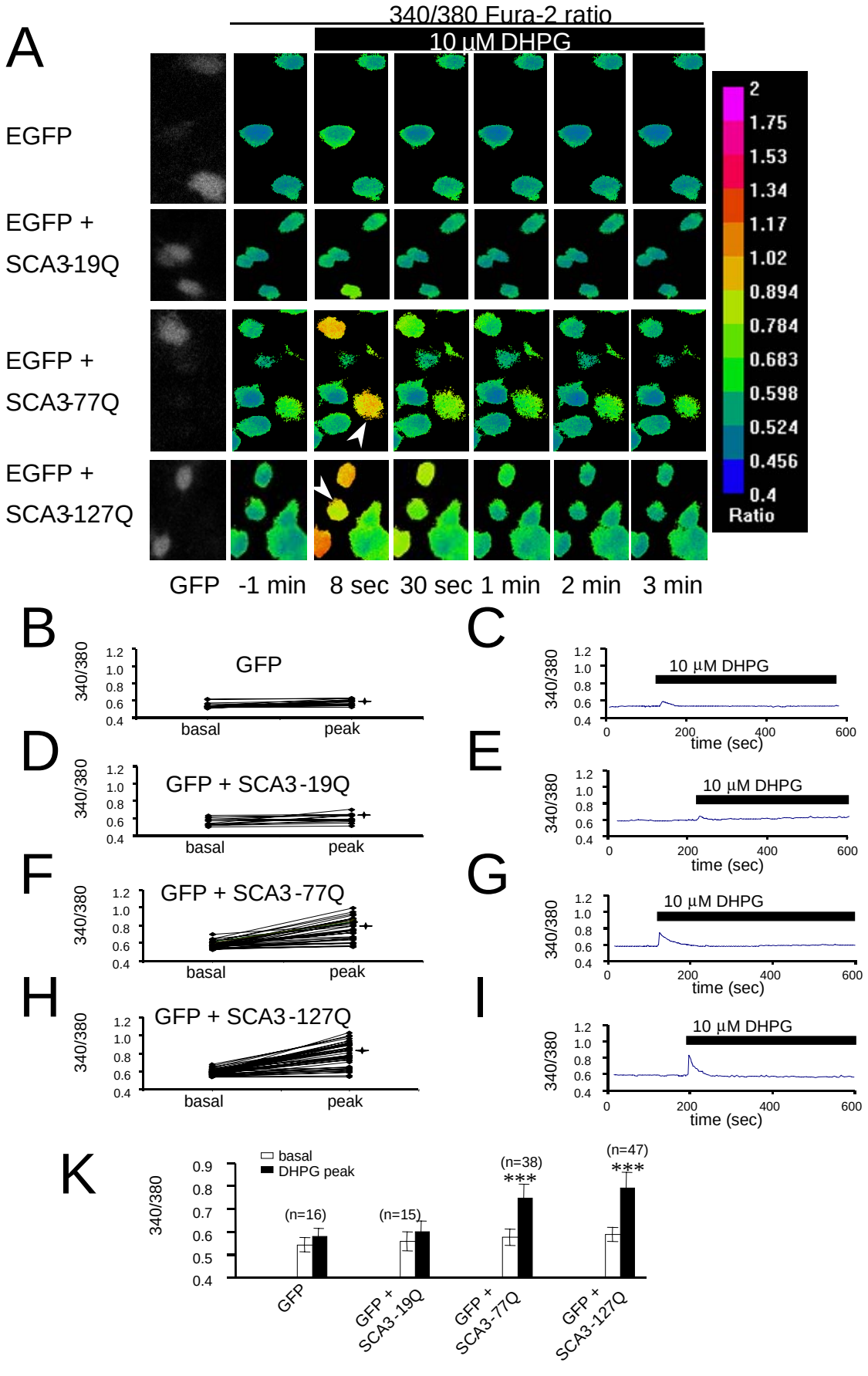
A
340/380 Fura-2 ratio
10 µM DHPG
EGFP
EGFP + SCA3-19Q
EGFP + SCA3-77Q
EGFP + SCA3-127Q
2
1.75
1.53
1.34
1.17
1.02
0.894
0.784
0.683
0.598
0.524
0.456
0.4
Ratio
GFP -1 min 8 sec 30 sec 1 min 2 min 3 min
B
GFP
C
10 µM DHPG
D
GFP + SCA3-19Q
E
10 µM DHPG
F
GFP + SCA3-77Q
G
10 µM DHPG
H
GFP + SCA3-127Q
I
10 µM DHPG
340/380
basal
peak
time (sec)
K
basal
DHPG peak
(n=16)
(n=15)
(n=38)
(n=47)
***
GFP
GFP + SCA3-19Q
GFP + SCA3-77Q
GFP + SCA3-127Q

Fig 2

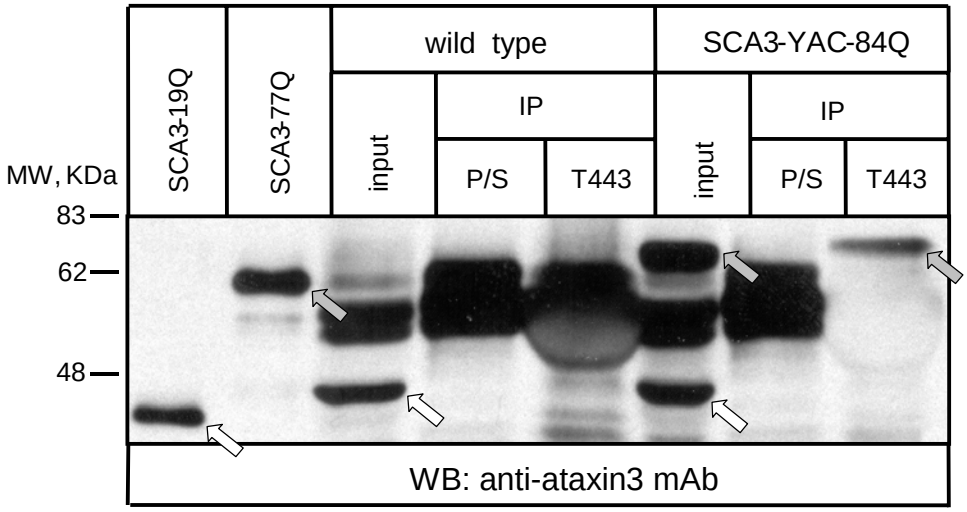
SCA3-19Q
SCA3-77Q
wild type
SCA3-YAC-84Q
input
IP
P/S
T443
input
IP
P/S
T443
MW, KDa
83
62
48
WB: anti-ataxin3 mAb

Fig 3

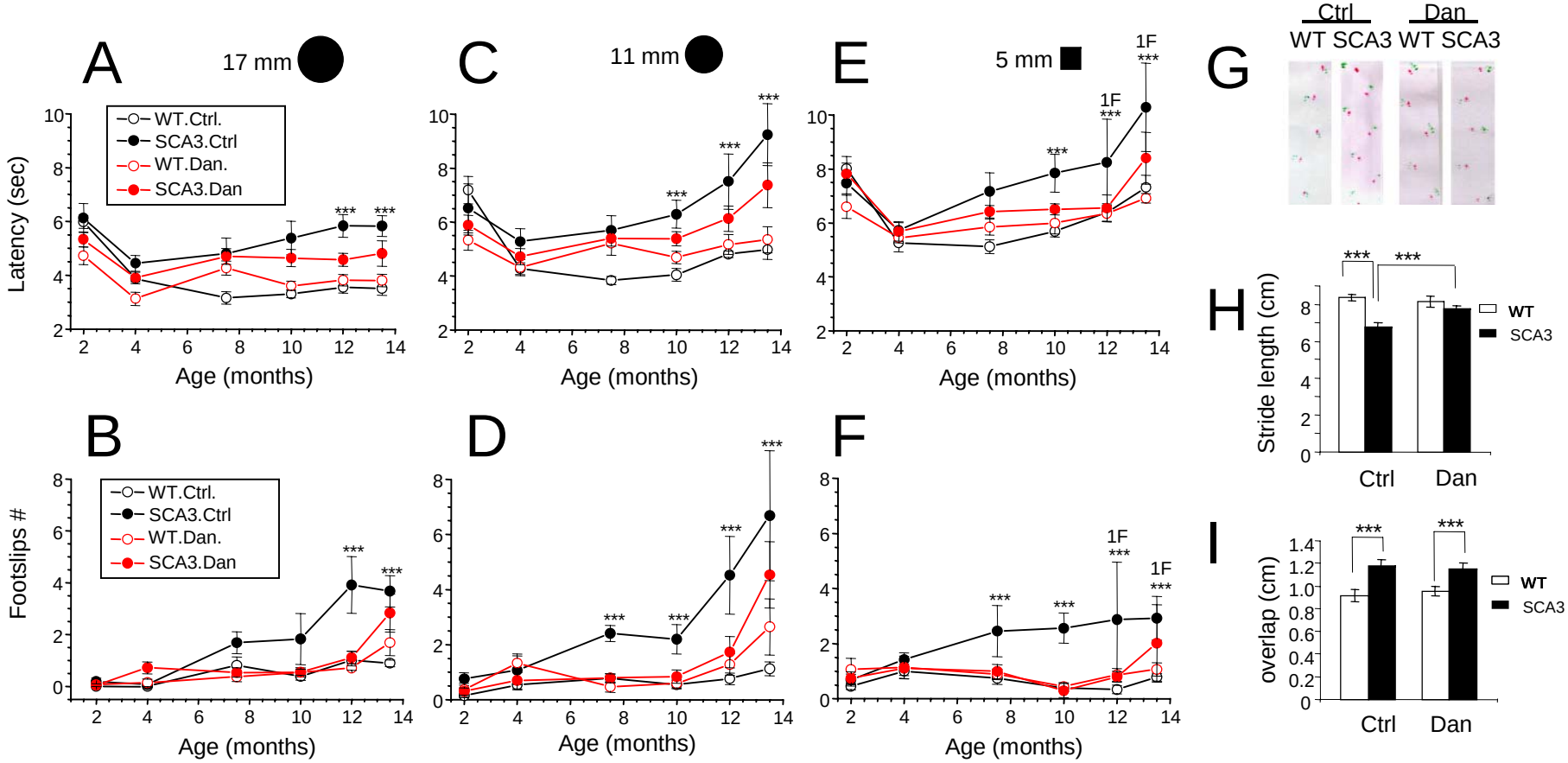
A
17 mm
C
11 mm
E
5 mm
WT.Ctrl.
SCA3.Ctrl
WT.Dan.
SCA3.Dan
Latency (sec)
Age (months)
B
D
F
Footslips #
1F
***
G
Ctrl
Dan
WT SCA3 WT SCA3
H
Stride length (cm)
WT
SCA3
Ctrl
Dan
I
overlap (cm)

Fig 4

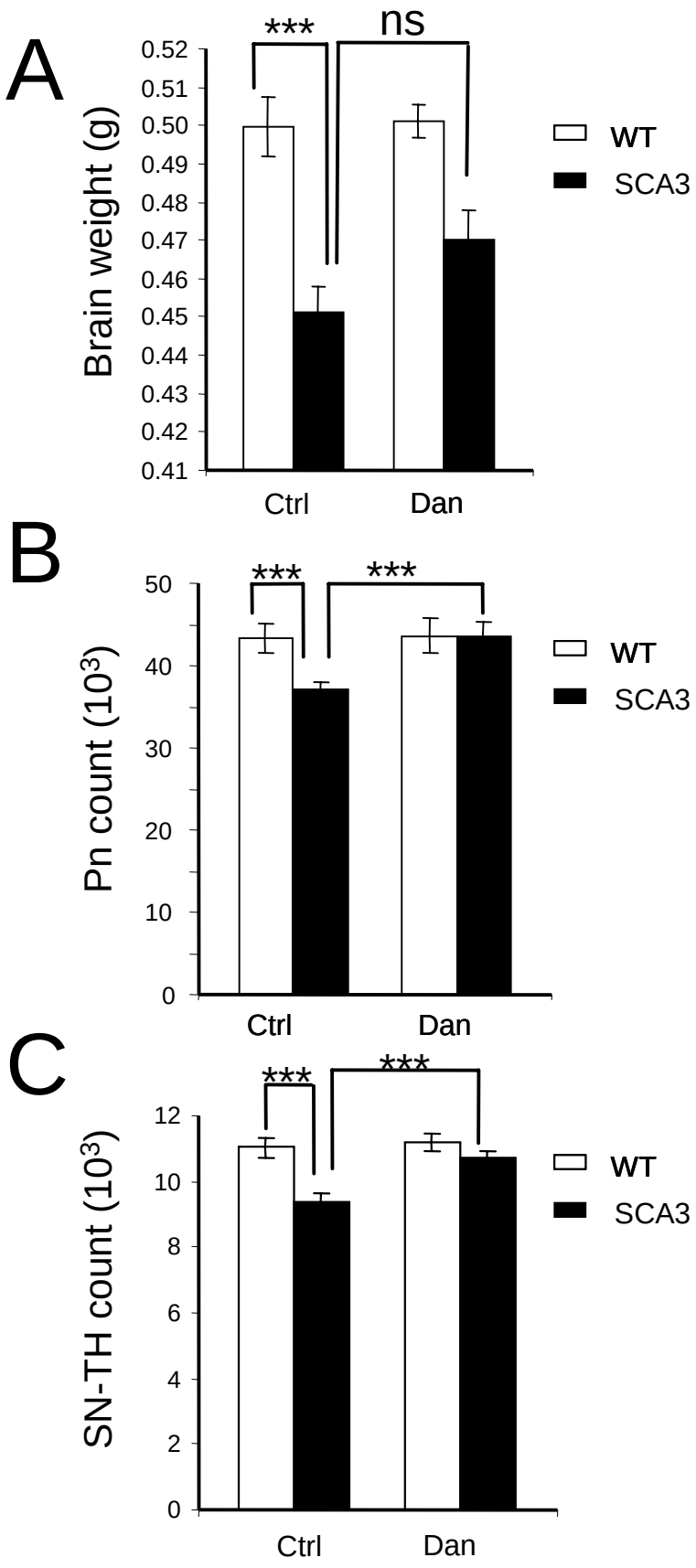
A
***
ns
0.52
0.51
0.50
0.49
0.48
0.47
0.46
0.45
0.44
0.43
0.42
0.41
Brain weight (g)
Ctrl
Dan
WT
SCA3
B
***
***
50
40
30
20
10
0
Pn count (10³)
Ctrl
Dan
WT
SCA3
C
***
***
12
10
8
6
4
2
0
SN-TH count (10³)
Ctrl
Dan
WT
SCA3

Fig 5